UT-BATTELLE

In-situ Scattering Study of Phase Transformation Kinetics

Xun-Li Wang

Neutron Scattering Science Division

Oak Ridge National Laboratory

Outline

- **Why are phase transformations of interest?**
- **Why kinetics?**
- **How are neutrons used to study phase transformations?**
- **Future opportunities**

The structure of a material at various length scales

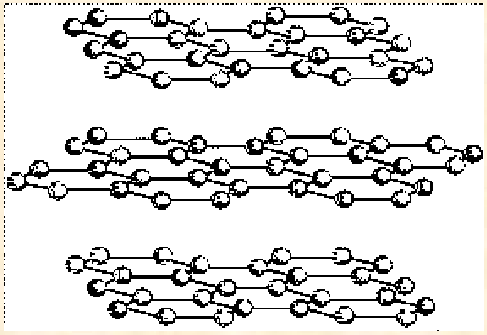

Graphite

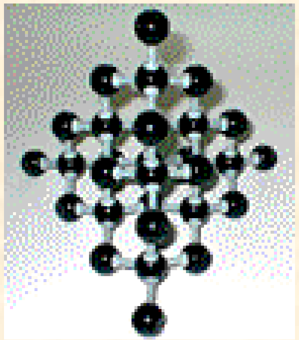

Diamond

Metallic Glass

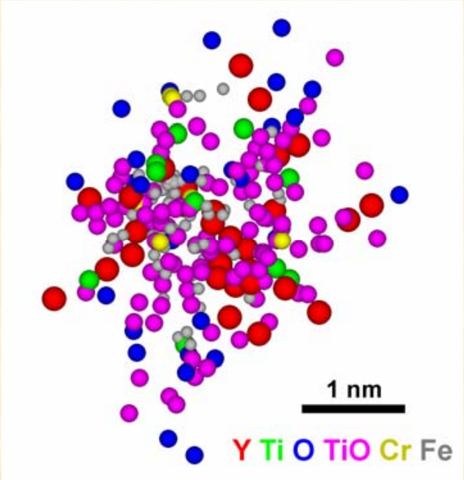

Nanoscale clusters

Nanocrystalline Ni

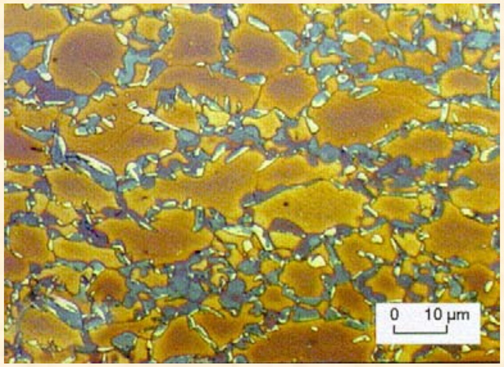

TRIP Steel

UT-BATTELLE

Structure Affects Properties

Structural change during curing of cement

(Chakomakous et al., Acta Cryst. 1992)

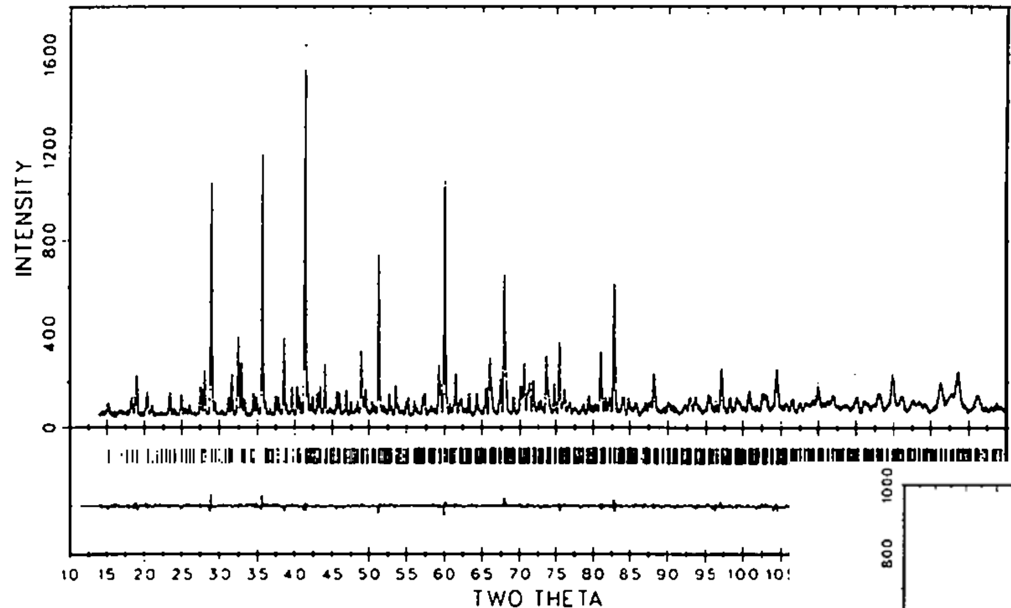

Fig. 1. Observed, calculated and difference neu
fraction profiles for $Sr_3Al_2O_6$. The observed d
by dots and the calculated profile is the contin
the same field. The short vertical lines below
the positions of all possible Bragg reflections,
curve is the difference between the observe
intensity (plotted using the same vertical scale
and calculated profiles).

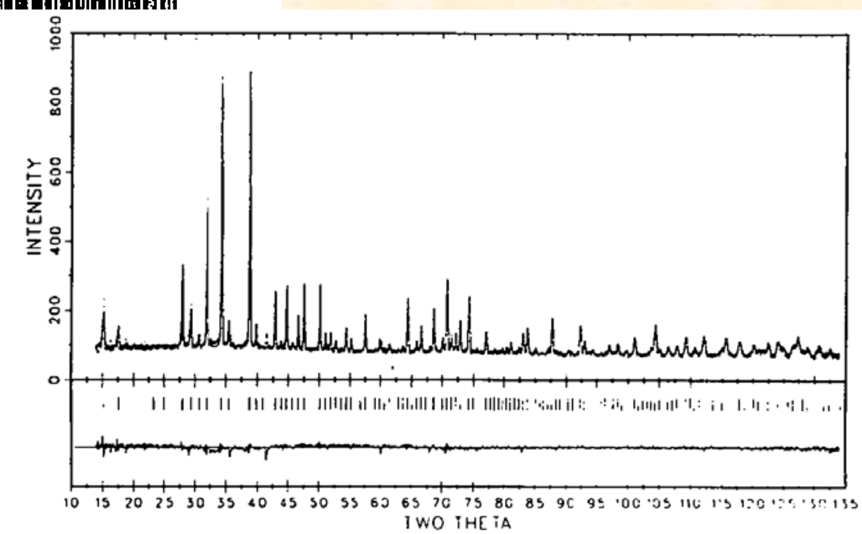

Fig. 3. Observed, calculated, and difference neutron powder diffraction profiles for $Sr_3Al_2(O_4D_4)_3$. The description of the profiles is the same as Fig. 1.

Structure of metallic glass?

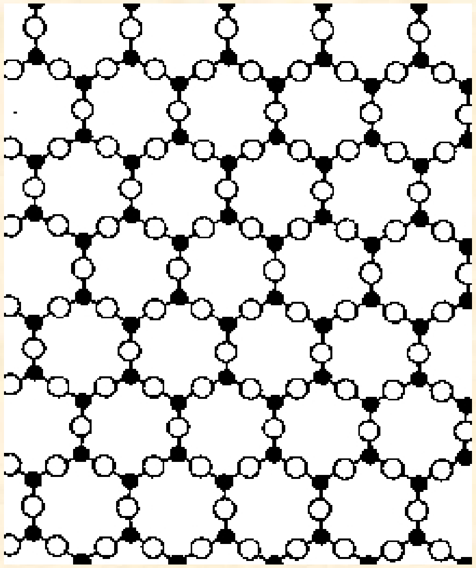

crystalline

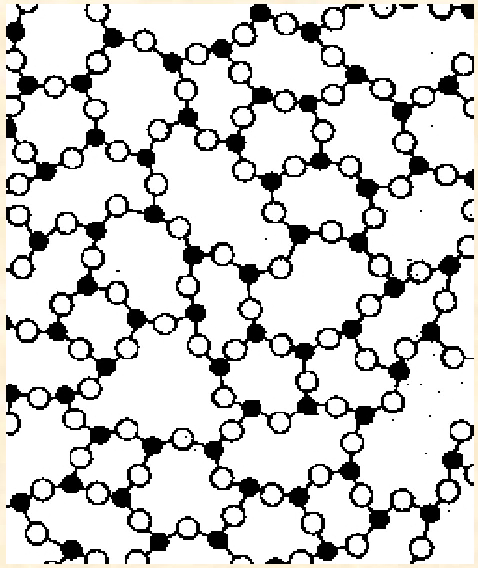

amorphous?

Miracle, Nature Mat.

The structure of a material at various length scales

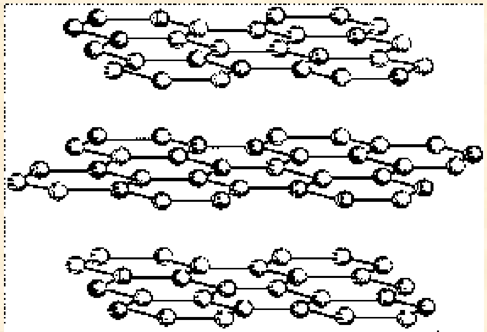

Graphite

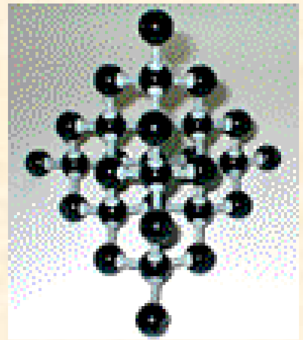

Diamond

Metallic Glass

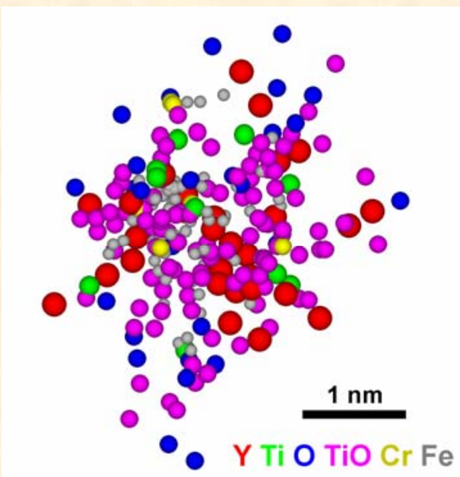

Nanoscale clusters

Nanocrystalline Ni

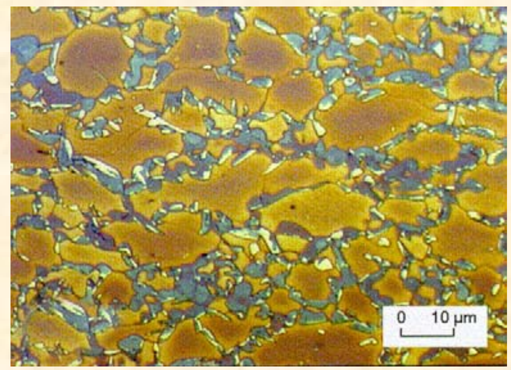

TRIP Steel

UT-BATTELLE

New 12YWT Nanocomposited Ferritic Steel has Superior Strength compared to conventional ODS steels

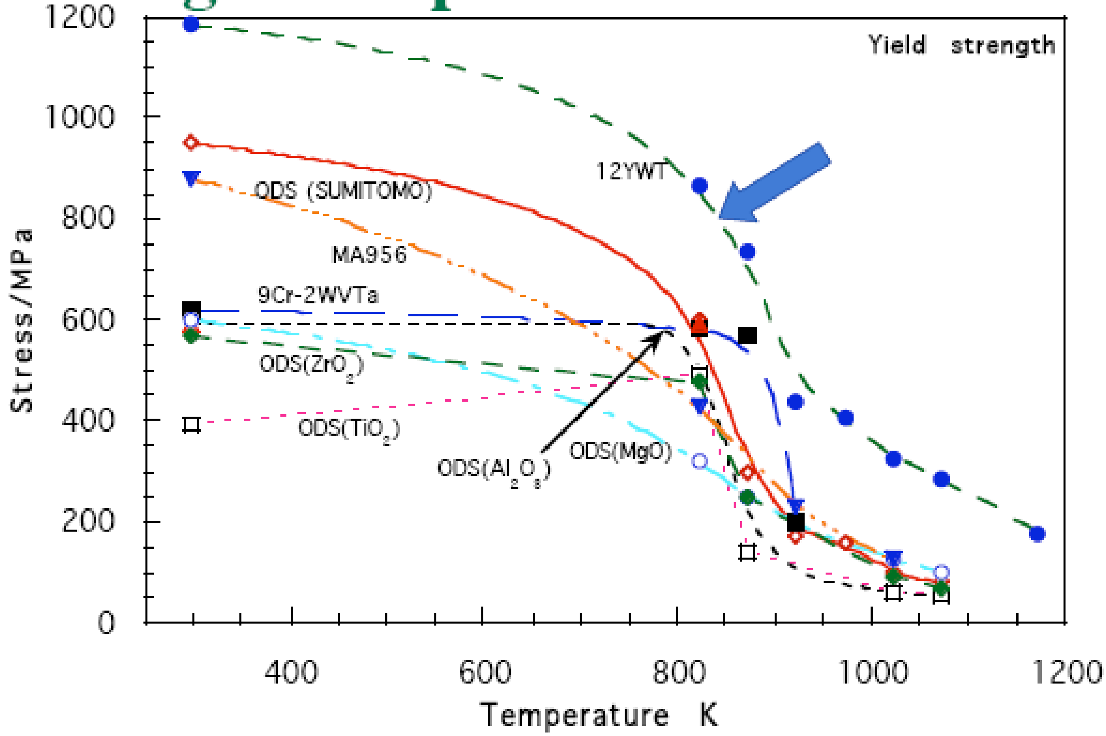

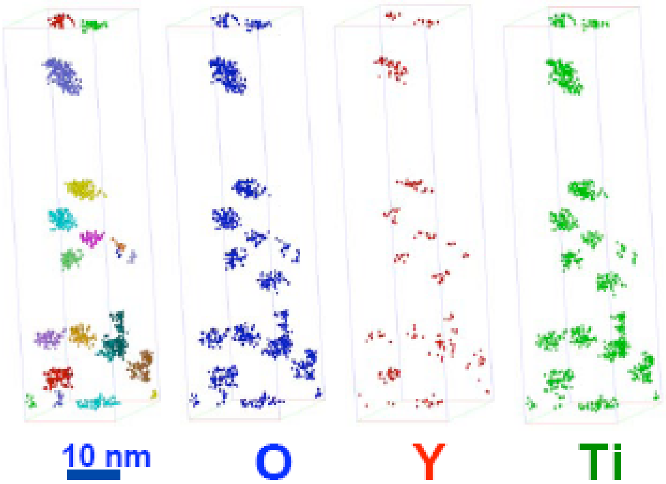

- Thermal creep time to failure is increased by several orders of magnitude at 800°C compared to ferritic/martensitic steels
- Potential for increasing the upper operating temperature of iron based alloys by ~200°C
- Acceptable fracture toughness near room temperature

- Atom Probe reveals nanoscale clusters to be source of superior strength
  - Enriched in O(24 at%), Ti(20%), Y (9%)
  - Size : $r_g = 2.0 \pm 0.8$ nm
  - Number Density : $n_v = 1.4 \times 10^{24}/m^3$
- Original Y_2O_3 particles convert to thermally stable nanoscale (Ti,Y,Cr,O) particles during processing
- Nanoclusters not present in ODS Fe-13Cr + $0.25Y_2O_3$ alloy

D.J. Hoelzer et al.

NANOCLUSTERS IN IRON MATRIX

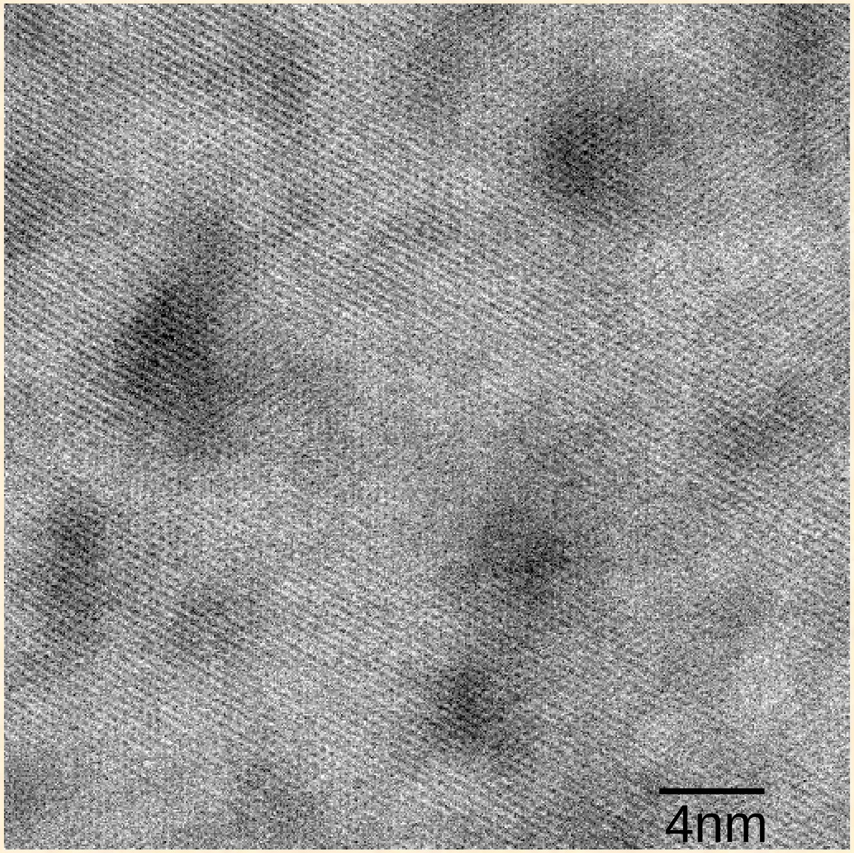

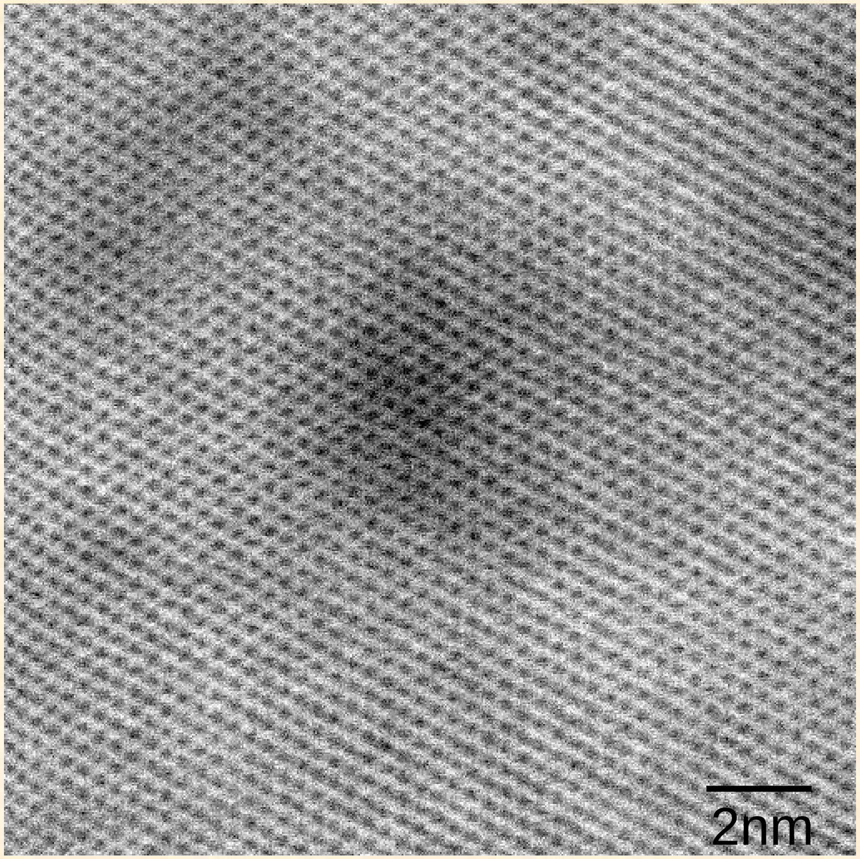

The nanoclusters were estimated to be 2-3 nm in diameter with a spacing of 12 nm in agreement with APT.

14YWT 1 h at 1000°C

Small Angle Neutron Scattering showed a bi-modal size distribution

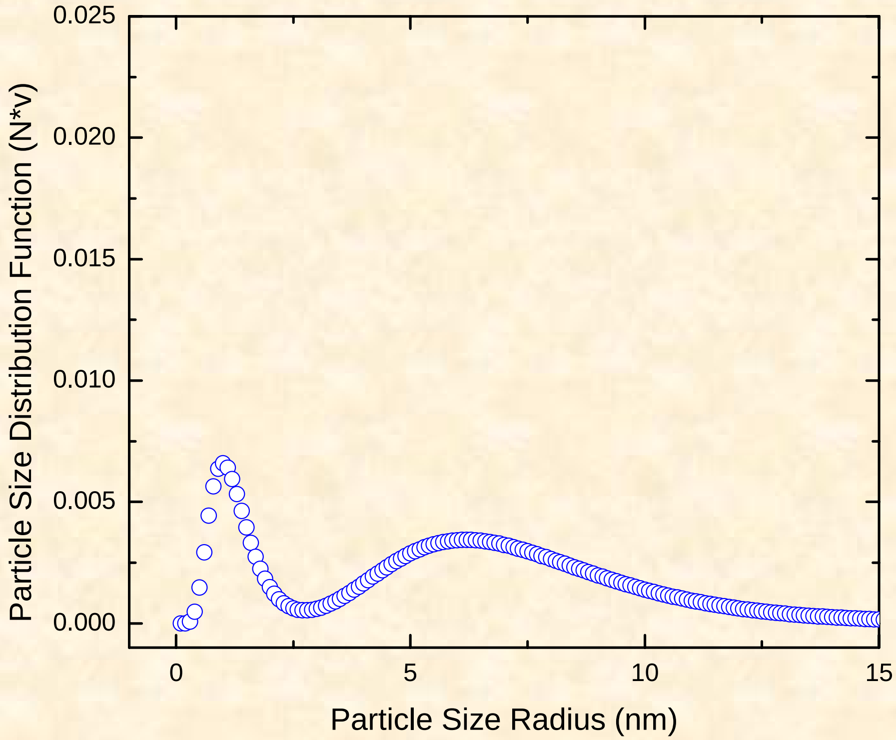

and thermally stable up to 1400 C

Structure Determines Properties - Microstructure

Cross-section of a friction stir weld showing distinct microstructure zones generated by heat and mechanical work

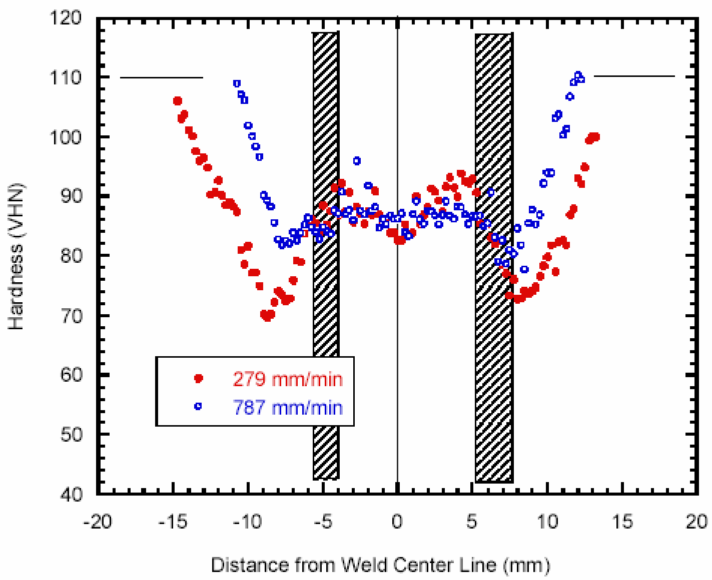

Hardness profile through the different microstructure zones reflects the changes in microstructure

Wang et al., 1999

UT-BATTELLE

Microstructure of TRIP Steel

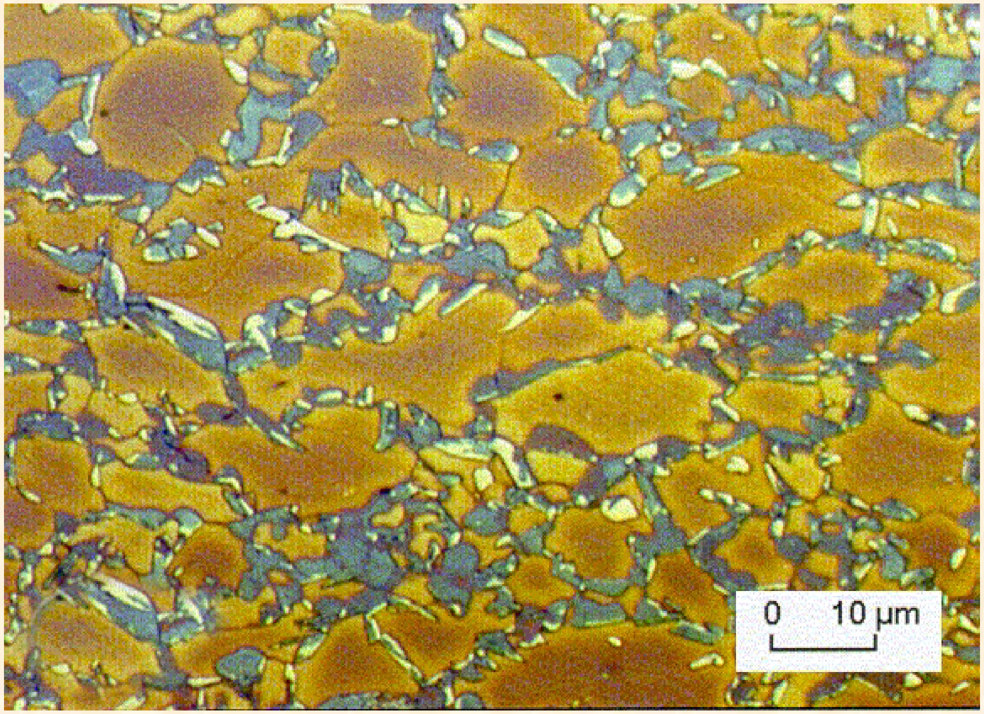

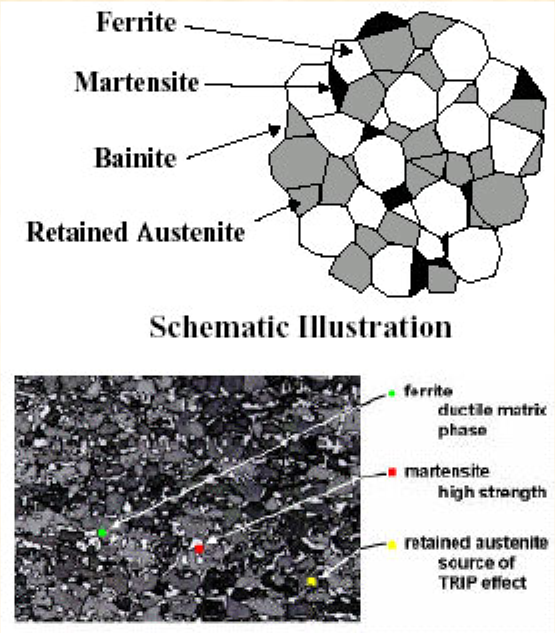

- TRansformation Induced Plasticity steels
- Retained austenite transforms into martensite (a hard phase) during deformation
- Hard martensite delays the onset of necking resulting in high total elongation
- Extremely high fatigue endurance

Why Kinetics?

- **Because we must !**
  - **Mechanisms of nucleation**
  - **Mechanisms of growth**
  - **Nature of intermediate and meta-stable phase**
  - **…**

  - **Ultimate goal is achieve structure control**
  - **Effect on properties**
- **Because we can !**
  - **In-situ time-resolved measurements**

What we are interested in are evolution of the structures at multiple length scales

Length & Time

Examples

- Kinetic study of order-disorder phase transformation in Ni_3Mn (1986)
- Kinetic study of $\alpha \rightarrow \beta$ phase transformation in Mn (1999)
- Fatigue-induced phase transition (on-going)
- Transient behavior during welding
- Crystallization of bulk metallic glass

How are neutrons used to determine structures?

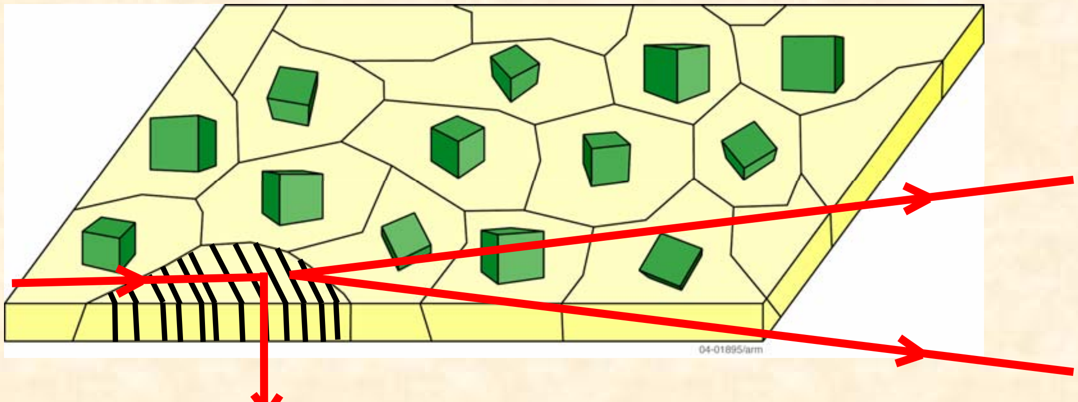

small angle scattering

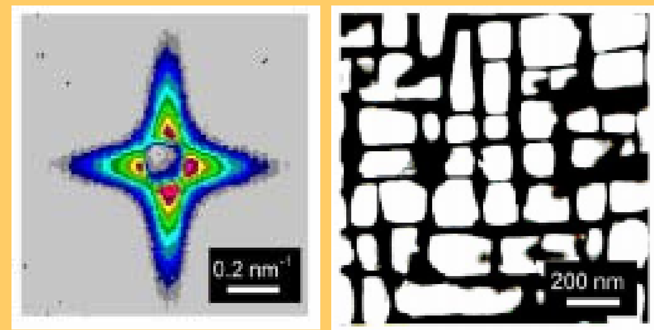

Grain morphology and size distribution

Ni (Al, Fe)

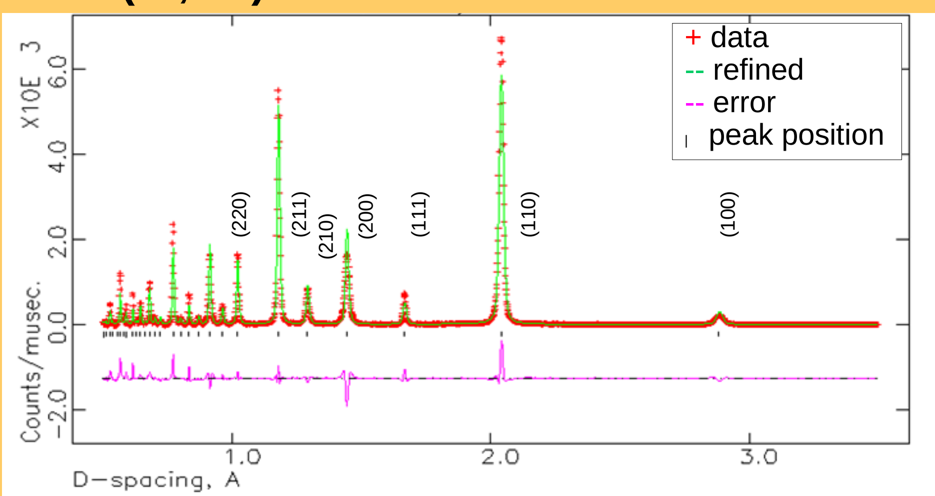

wide angle diffraction

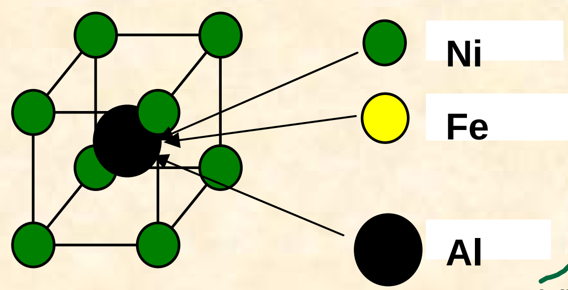

UT-BATTELLE

Order-disorder phase transformation in Ni_3Mn

- **Very difficult to study with X-ray**
  - **Mn Z=25**
  - **Ni Z=28**
- **Ideal for neutrons**
  - **Ni b=10.3 fm**
  - **Mn b=-3.8 fm**
- **Tc=510 C**

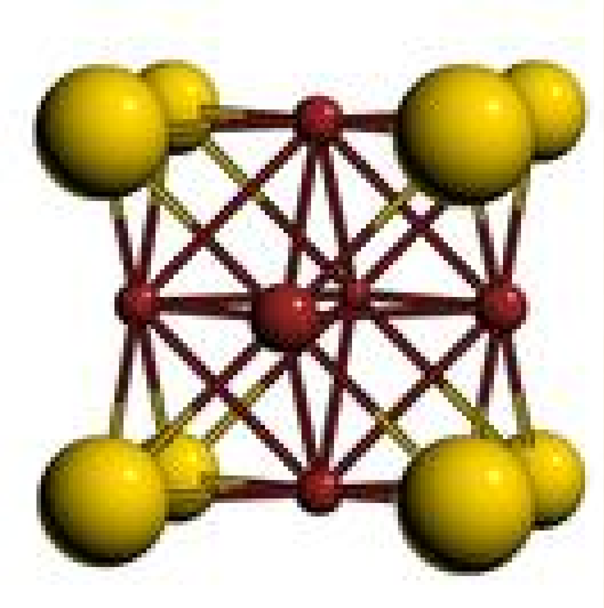

Real-time measurements – peak width

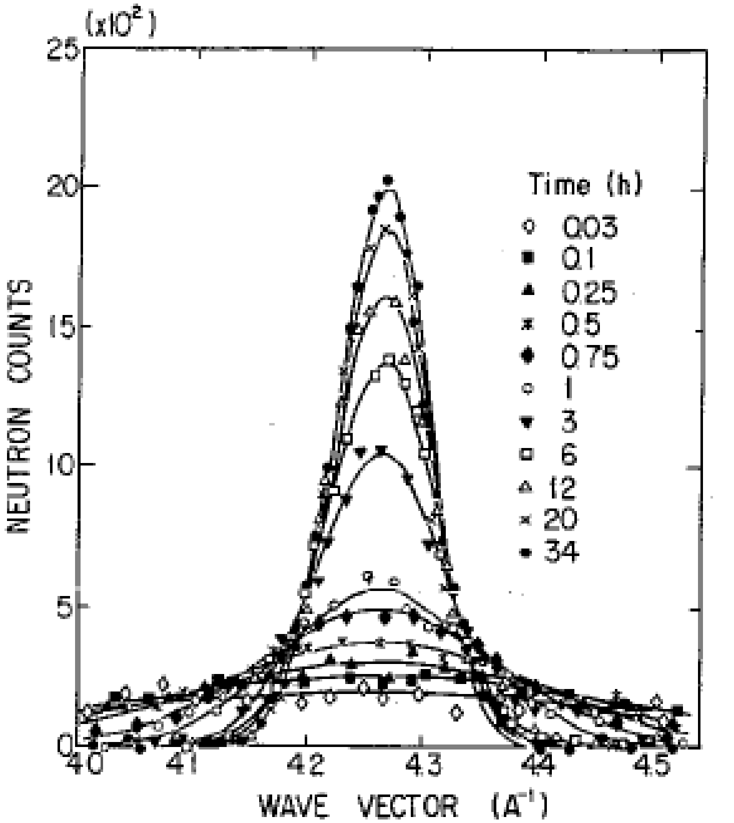

Fig 5. Time change of the 211 superlattice peak of Ni_3Mn

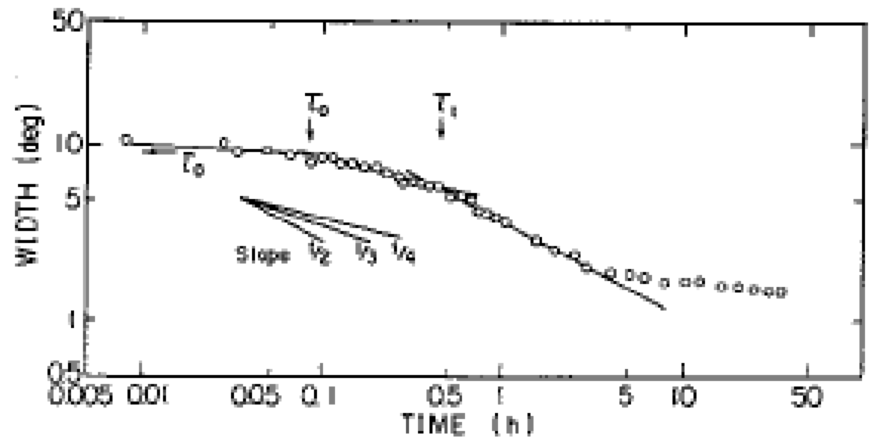

Fig 6. Change of the width of the 211 sublattice peak with time

(211) reflection

Kinetic study of α→β phase transformation in Mn

Real-time kinetic neutron powder diffraction study of the phase transition from α-Mn to β-Mn

J R Stewart† and R Cywinski
School of Physics and Astronomy, University of St Andrews, North Haugh, St Andrews, Fife KY16 9SS, UK

Received 6 July 1999, in final form 10 August 1999

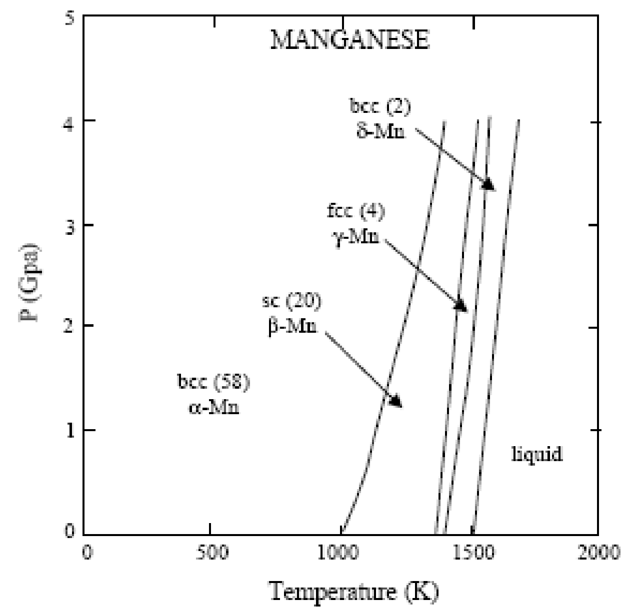

Figure 2. The phase diagram of manganese [2].

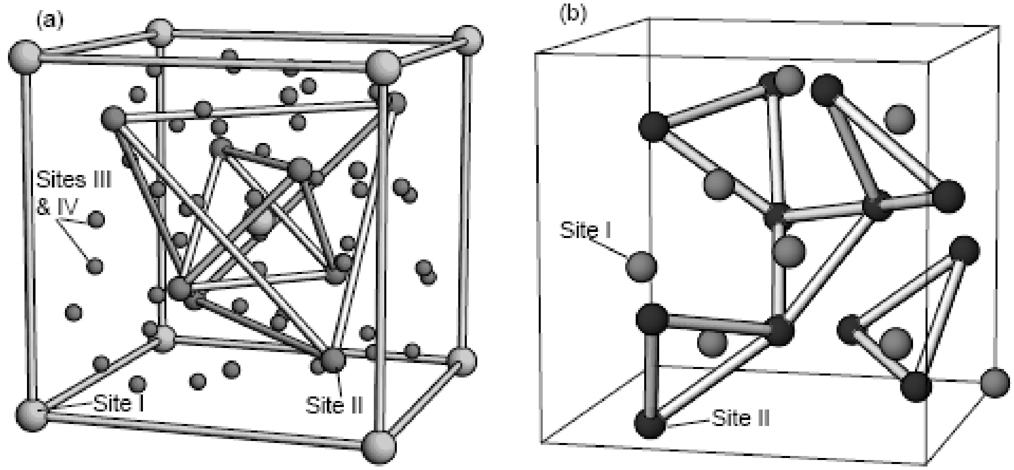

Figure 1. The (a) α-Mn and (b) β-Mn crystal structures.

UT-BATTELLE

Kinetic study of $\alpha \rightarrow \beta$ phase transformation in Mn

- **Experiments done on HRPD at ISIS**
  - **100 m instrument**
  - **Very high $\Delta d/d$ resolution of ~ 4×10^{-4}**

- **Time resolution: 5 minutes per data set**

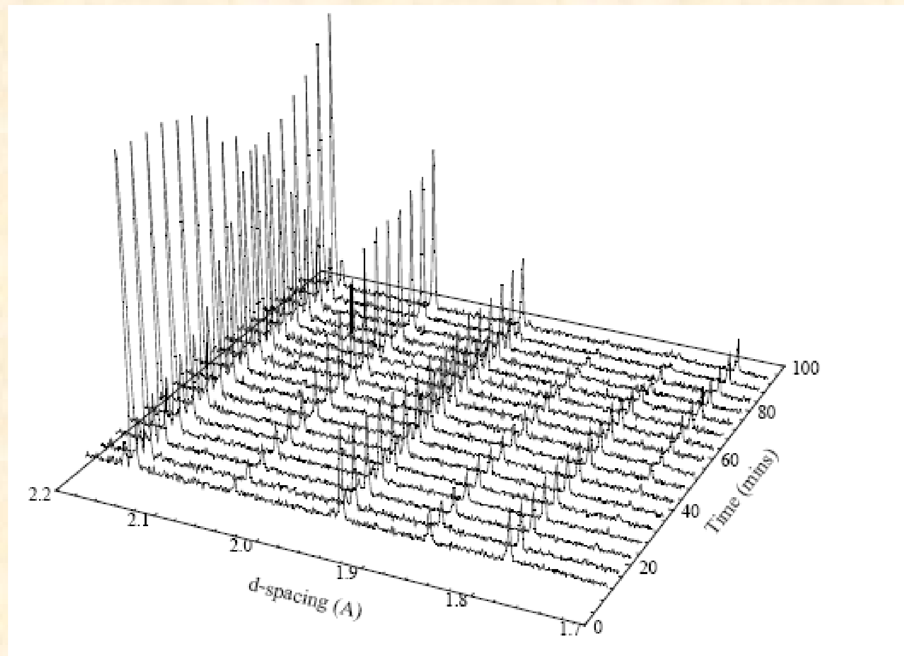

Figure 3. α-Mn to β-Mn phase transition at a temperature of 710 °C. The spectra shown represent ten-minute time slices.

Multiphase Rietveld analysis to yield volume fraction

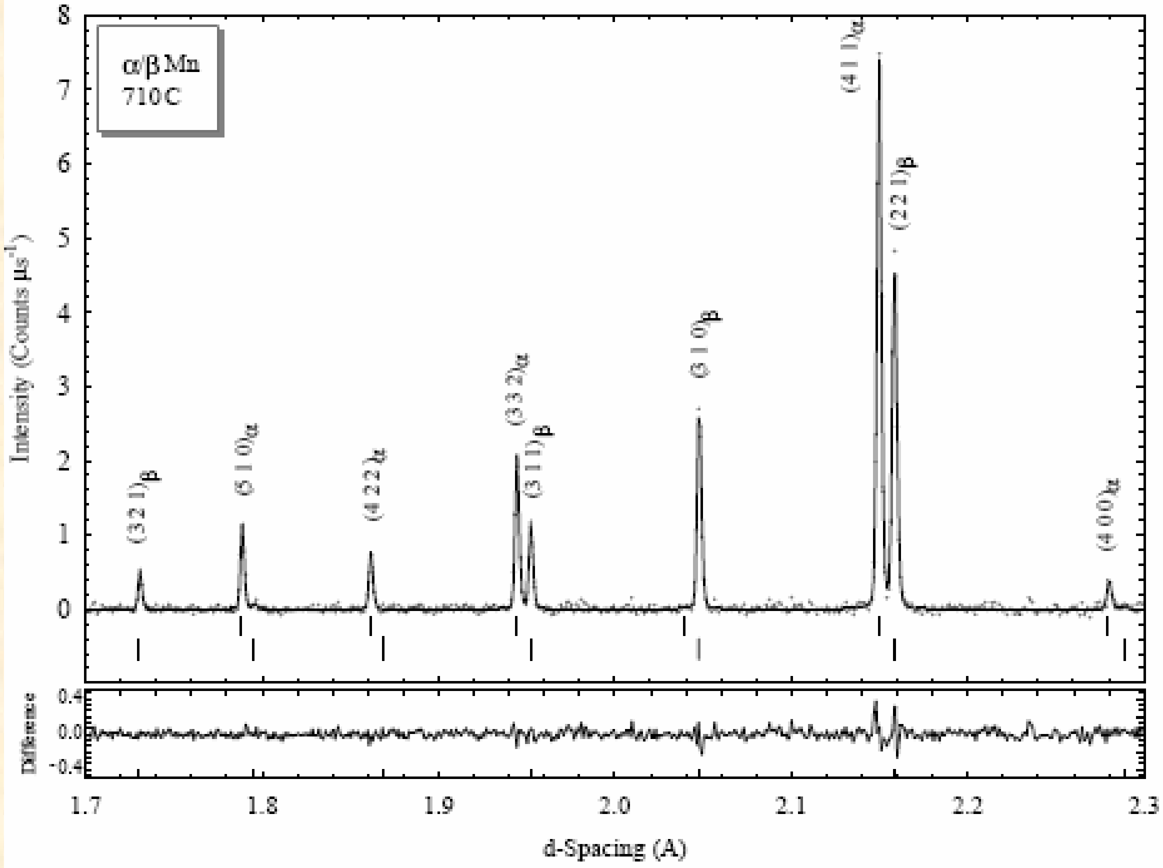

Figure 4. Typical two-phase Reitveld refinement of an α/β-Mn powder diffraction spectrum measured at 710 °C, and started 50 min into the measurement. The diffraction pattern was collected in 10 min. The α-Mn and β-Mn reflections are indicated by the subscripts shown in the figure.

Multiphase Rietveld analysis to yield volume fraction

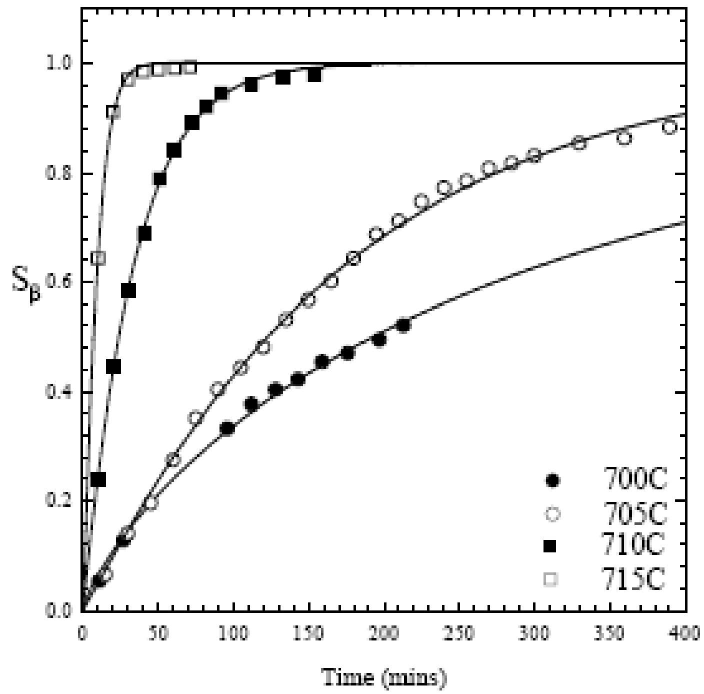

Figure 5. Measured time and temperature dependence of the β-Mn phase fraction S_β for the $\alpha-\beta$-Mn transition. The lines shown are fits to the AJM equation (3).

$$S_\beta = 1 - \exp[(-t/\tau)^n]$$

Tremendous difference in growth rates

Growth behavior follows scaling by Johnson-Mehl-Avrami theory

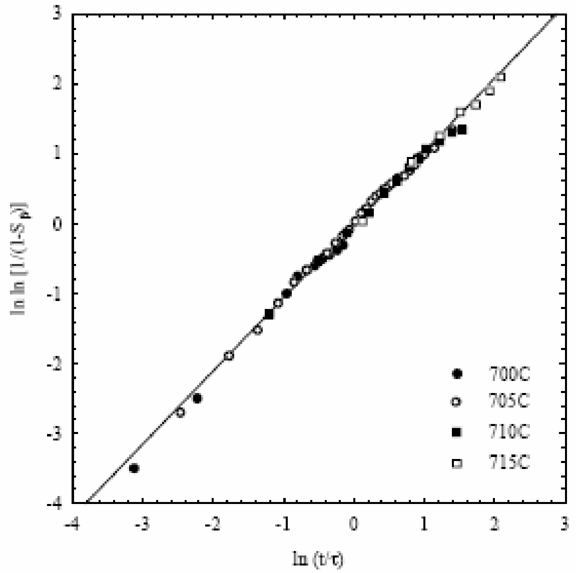

Figure 6. Graph of $\ln\ln(1/1 - S_\beta)$ against $\ln(t/\tau)$ demonstrating the scaling behaviour of the β-Mn phase fraction expressed in the form of a straight line of slope n. n is found to be 1.04 ± 0.02 for the α–β-Mn phase transition.

$$\ln\ln\left(\frac{1}{1 - S_\beta}\right) = n \ln\left(\frac{t}{\tau}\right)$$

Table 1. Type of growth process indicated by the exponent n in the AJM equation.

Exponent n	Type of growth
1	Homogeneous
$1 \leqslant n < 2$	One dimensional—*dendritic*
$2 \leqslant n < 3$	Two dimensional—*plate-like*
$3 \leqslant n < 4$	Three dimensional

Phase transformation induced by cyclic loading (fatigue)

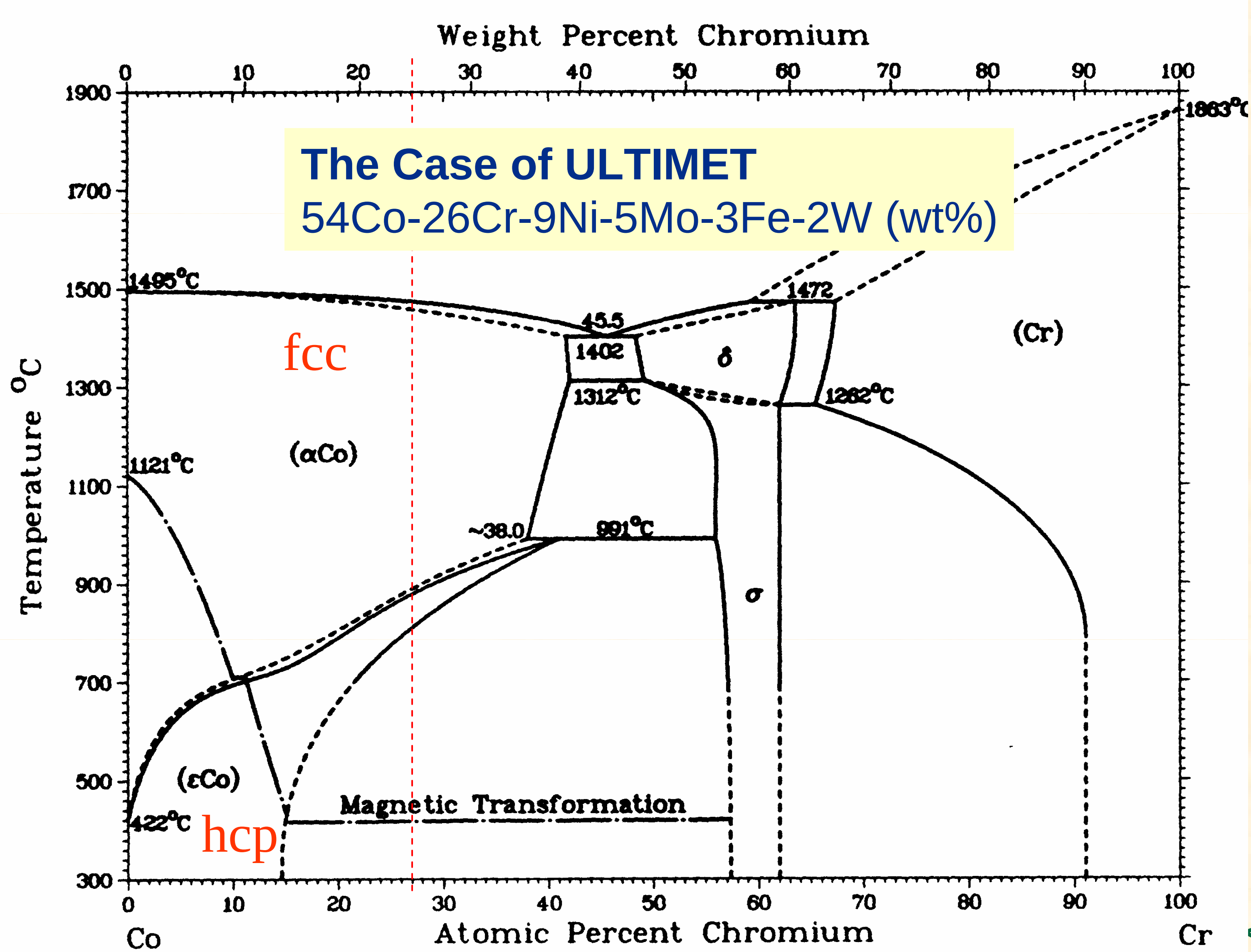

The Case of ULTIMET
54Co-26Cr-9Ni-5Mo-3Fe-2W (wt%)

***Source: Binary Alloy Phase Diagrams, ASM, Metals Park, OH, 1986, vol.1, p. 759.**

In-situ Neutron Diffraction

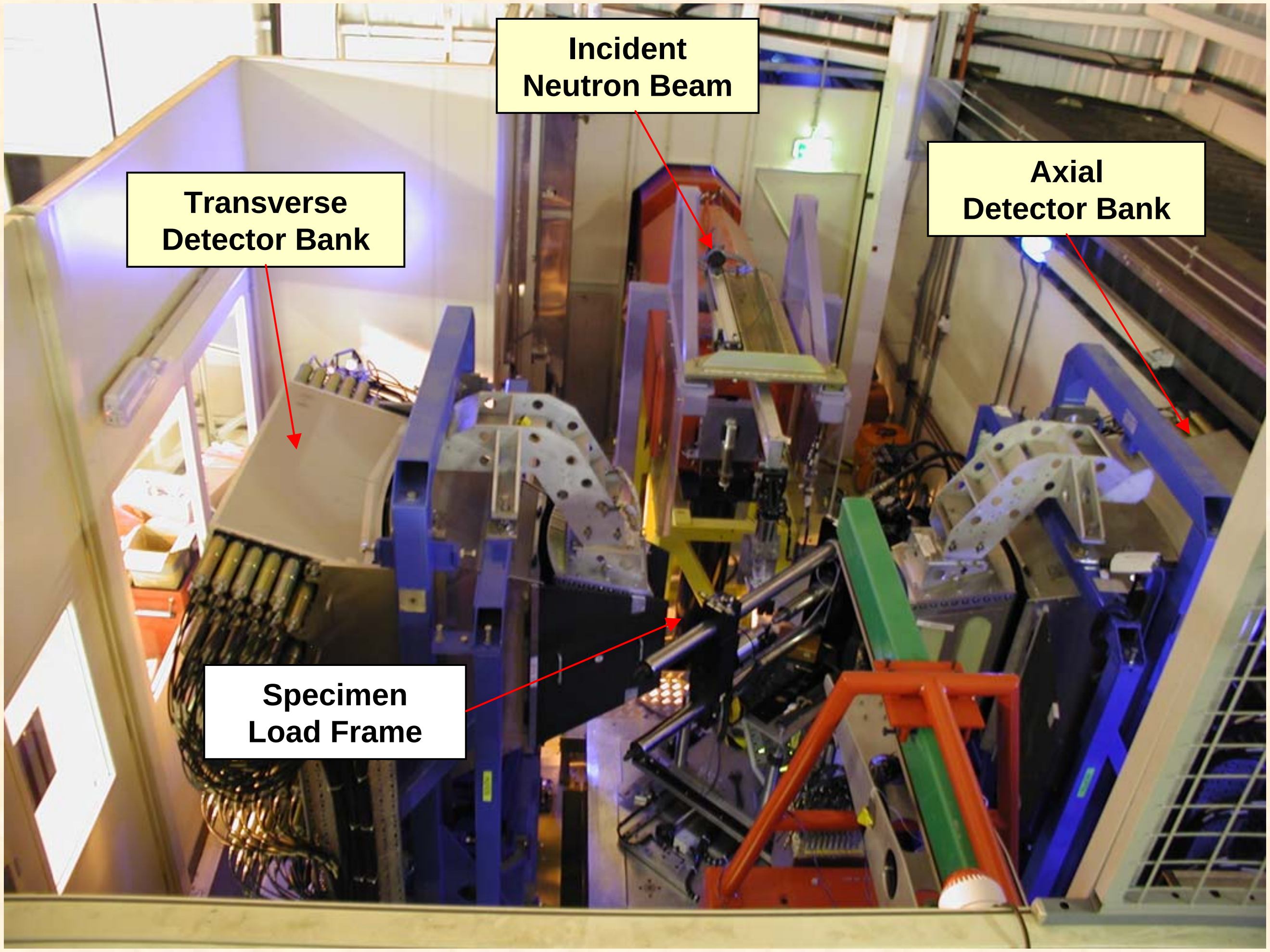

- ENGIN-X at the ISIS facility, UK.
- Pulsed neutron source.
- 40 minute count times, Co scatters poorly.
- Sampling volume: ~120 mm^3.

M. Benson et al., Powder Diffraction 2005

UT-BATTELLE

In-situ Neutron Diffraction

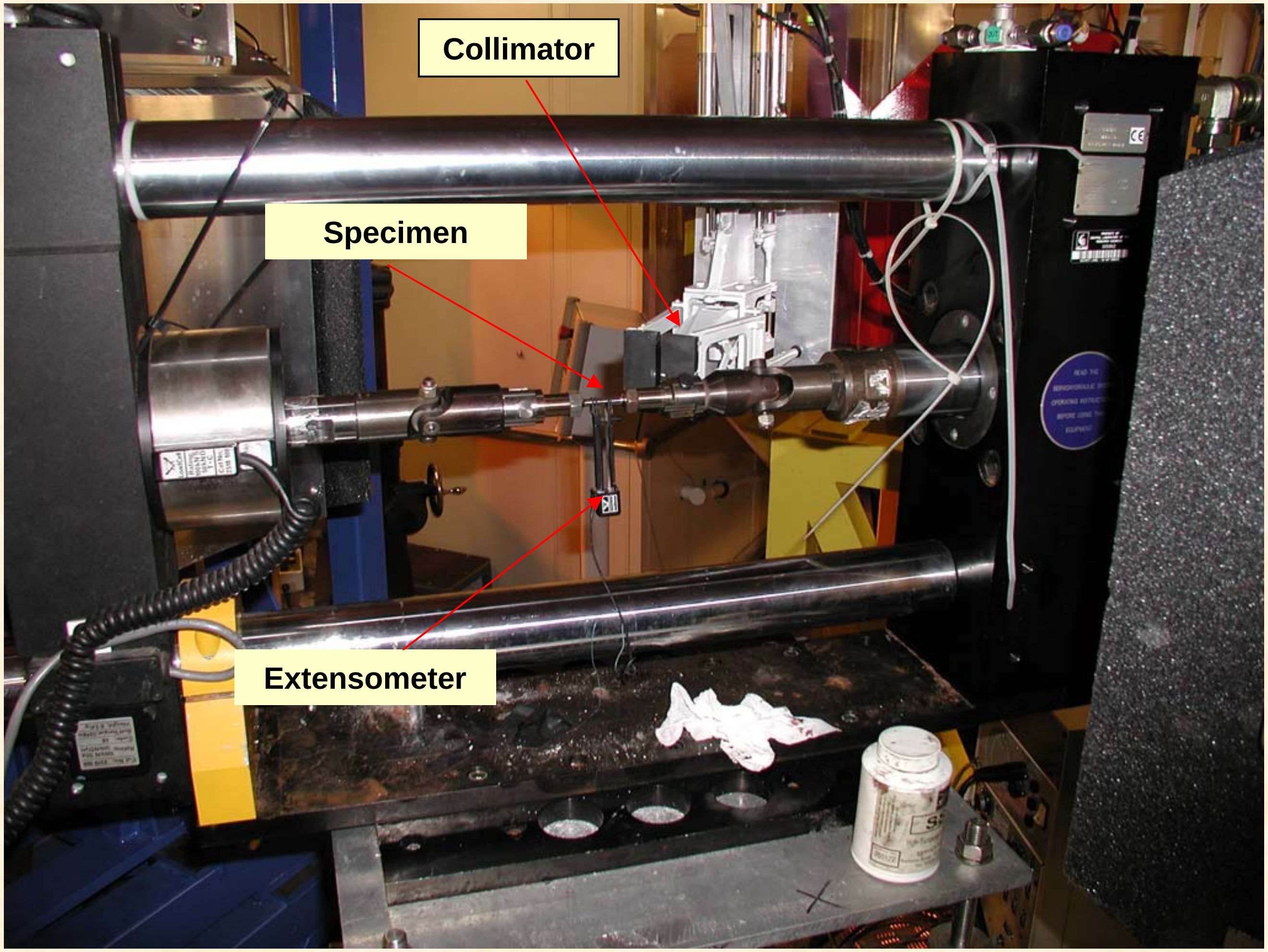

- Strain-controlled fatigue: R = -1, tension-compression (R is the ratio of the minimum strain to maximum strain).
- Total strain range, $\Delta\varepsilon = 2.5$ %.
- Cycling frequency, f = 0.5 Hz.
- Cylindrical specimens of 8 mm gage diameter, 24 mm gage length, M12 threaded ends.

M. Benson et al., Powder Diffraction 2005

UT-BATTELLE

Evolution of the hcp phase during fatigue test

Overlay of the axial detector bank diffraction patterns measured at “point 1.”

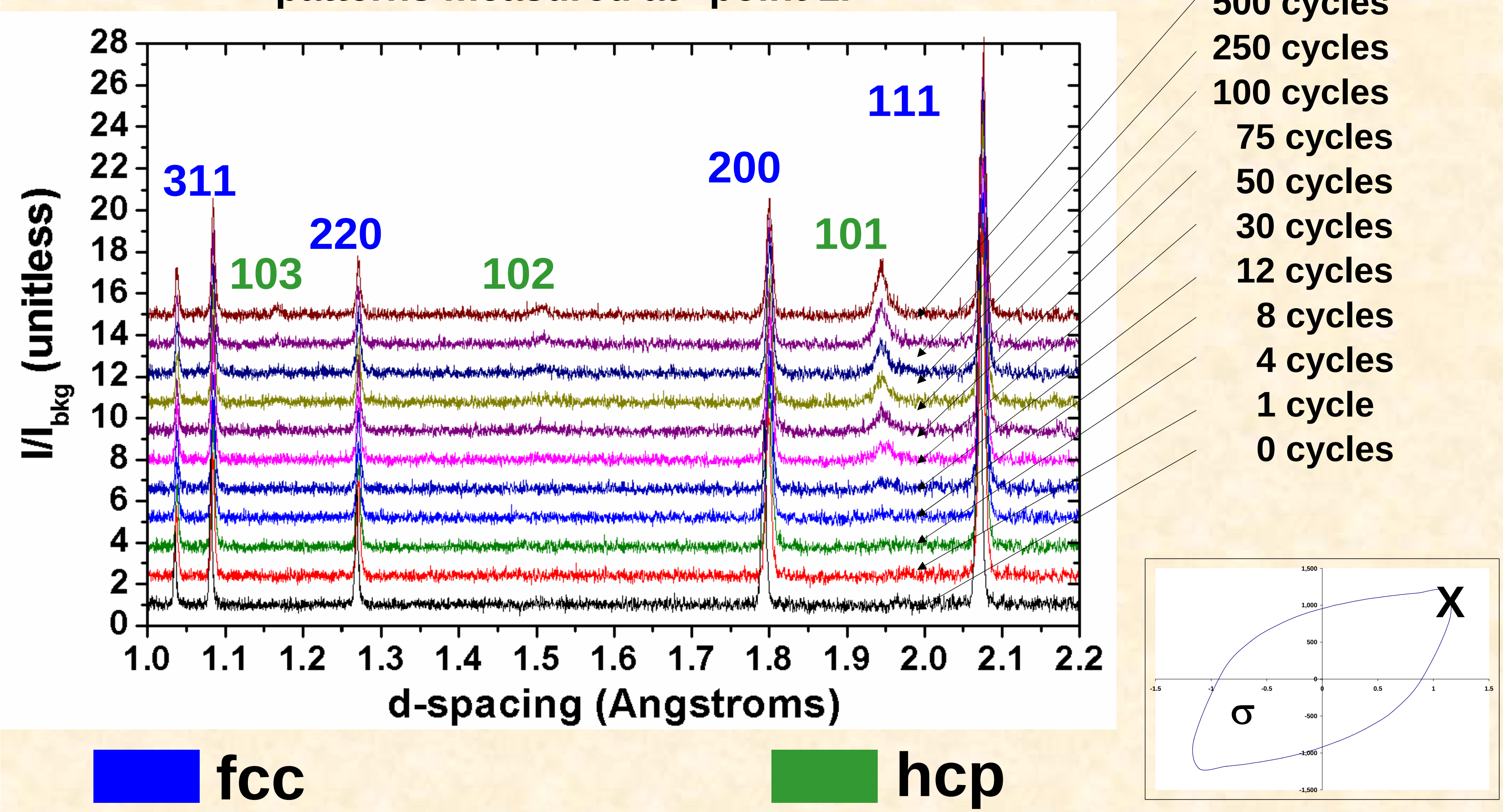

M. Benson et al., Powder Diffraction 2005

Increase in the HCP Peak Intensity as a Function of Fatigue Cycles

Increase in intensity of the hcp (101) peak.

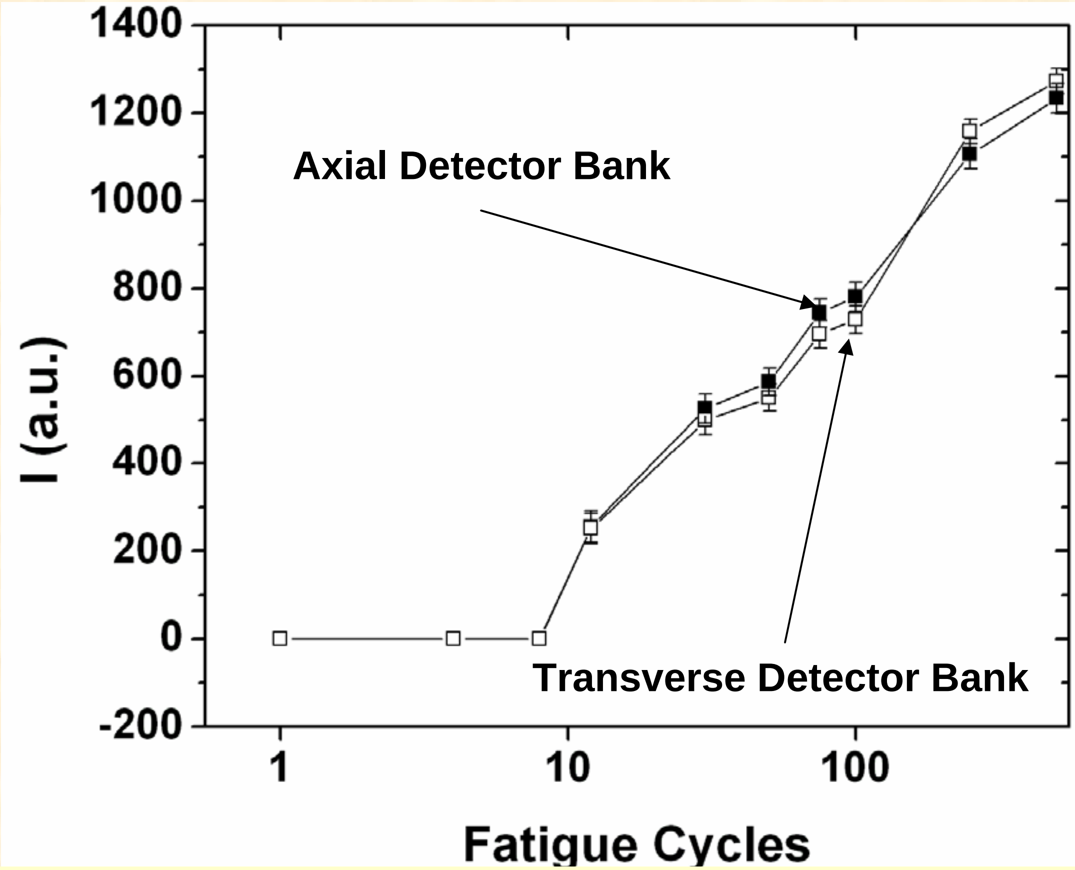

- Demonstrates the incubation period found in austenitic stainless steels during low cycle fatigue*.
- Demonstrates increase in volume fraction as fatigue progresses and strain accumulates.
- Similar trends in both the axial and transverse detector banks.
- Attributed to the interaction of stacking faults during low cycle fatigue.**

*** Source: ASM Handbook, Vol. 18. ASM International, 1997.**

****Source: L. Jiang, C. R. Brooks, P. K Liaw, J. Dunlap, C. J. Rawn, R. A. Peascoe, and D. L. Klarstrom, Met Trans A (2004) 35 3 785-796.**

UT-BATTELLE

Bulk Metallic Glass Materials Exhibit Unconventional Properties

- **Excellent mechanical properties**
- **Controllable magnetic properties**

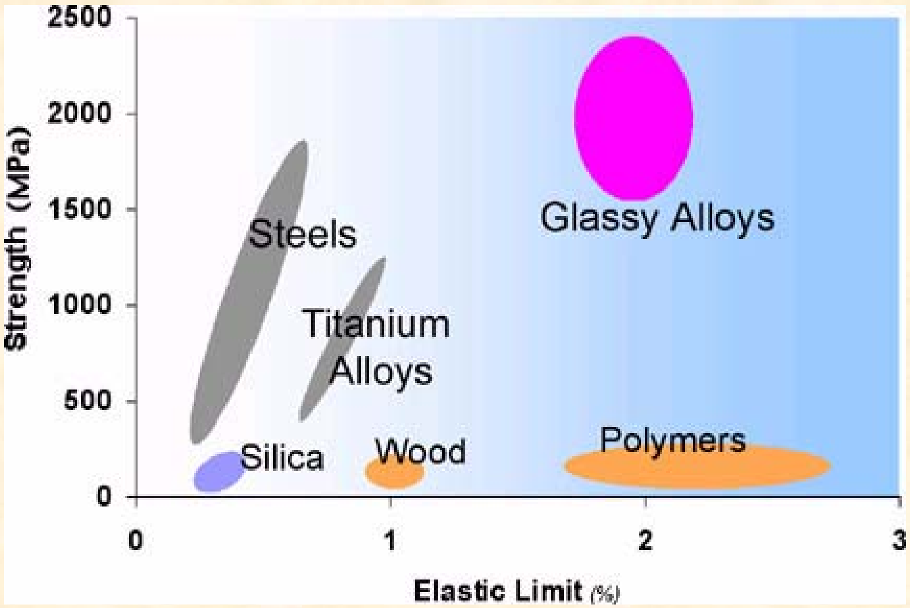

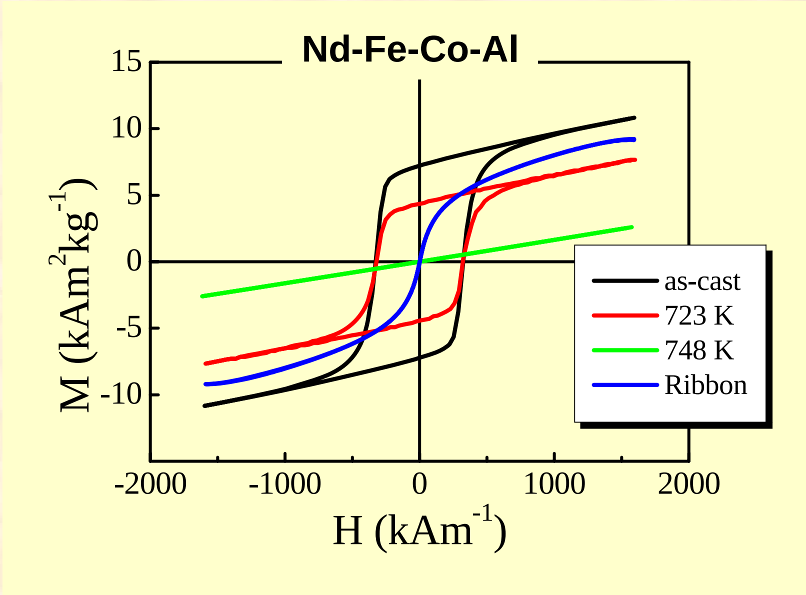

Partially Crystallized Bulk Metallic Glass Contains High-density Nanometer Sized Crystallites

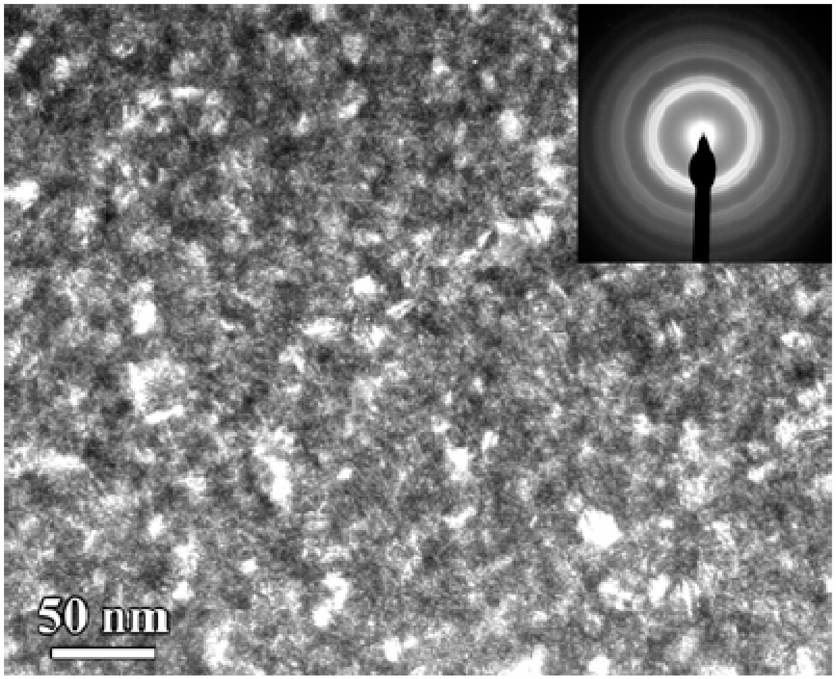

Figure 4
Dark-field transmission electron microscopy image with diffraction pattern (inset) of Vit105, annealed for 15 h at 673 K (Pekarskaya *et al.* 2003).

- **e.g., upon isothermal annealing**
- **Density 10^{23}-10^{24} m^{-3}**
- **Crystallite size ~10-50 nm**
- **Even for temperatures close to T_g**

Simultaneous Diffraction and Small Angle Scattering in Bulk Metallic Glass Show Concurrent Structural and Chemical Ordering

amorphous

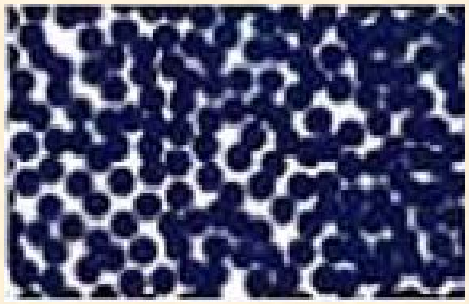

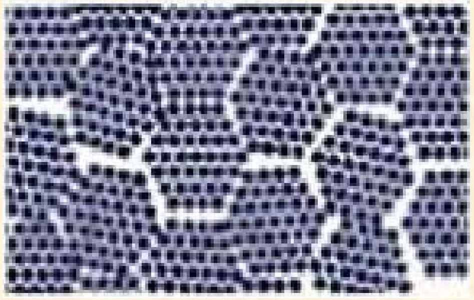

crystalline

Structural changes in two length scales

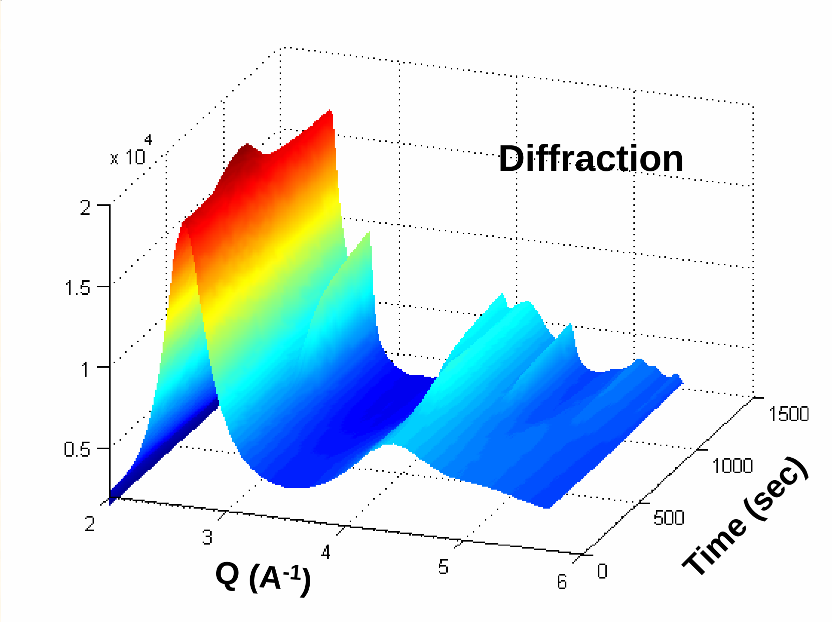

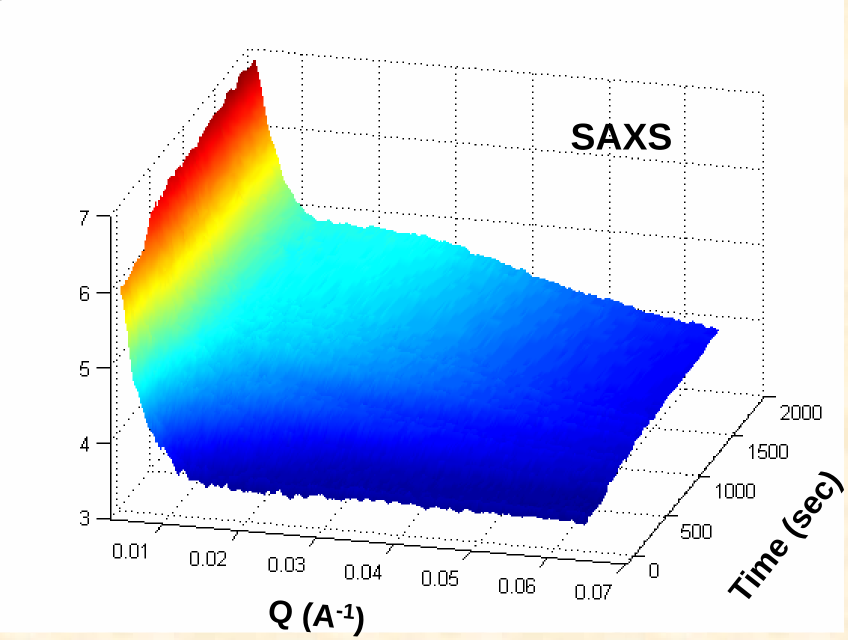

OAK RIDGE NATIONAL LABORATORY
U. S. DEPARTMENT OF ENERGY

Wang et al., Phys. Rev. Letter., 2003

Wang et al., unpublished

UT-BATTELLE

In-situ Neutron Diffraction Measurements Revealed for the first time Stress and Temperature Profiles during Friction Stir Welding

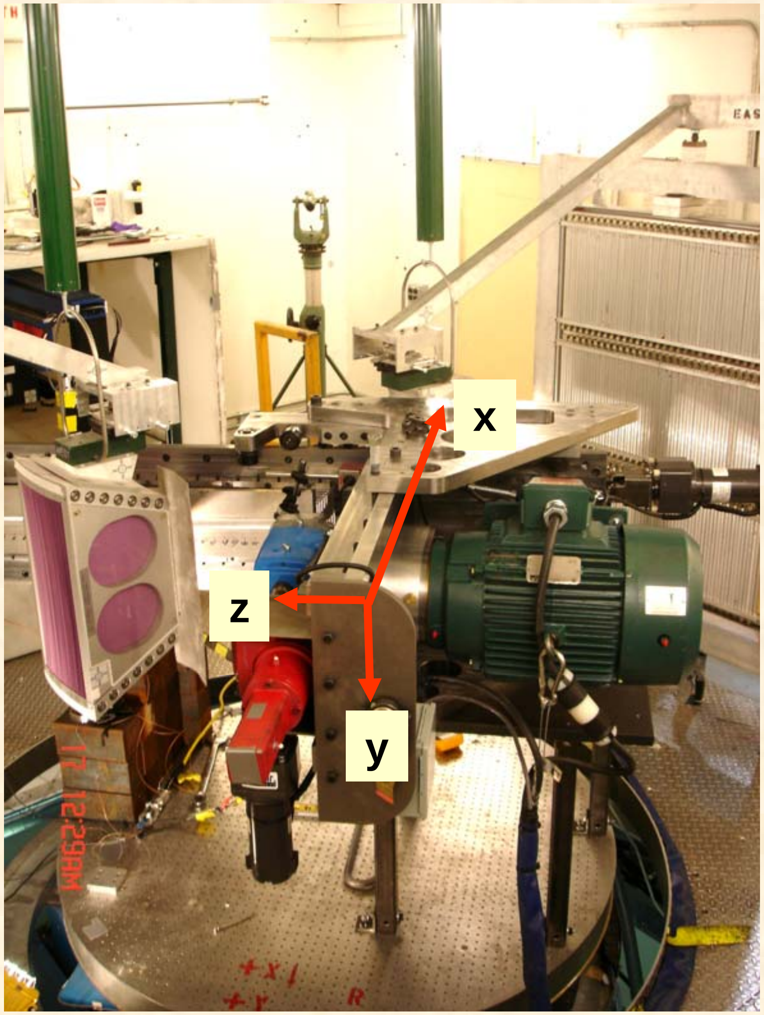

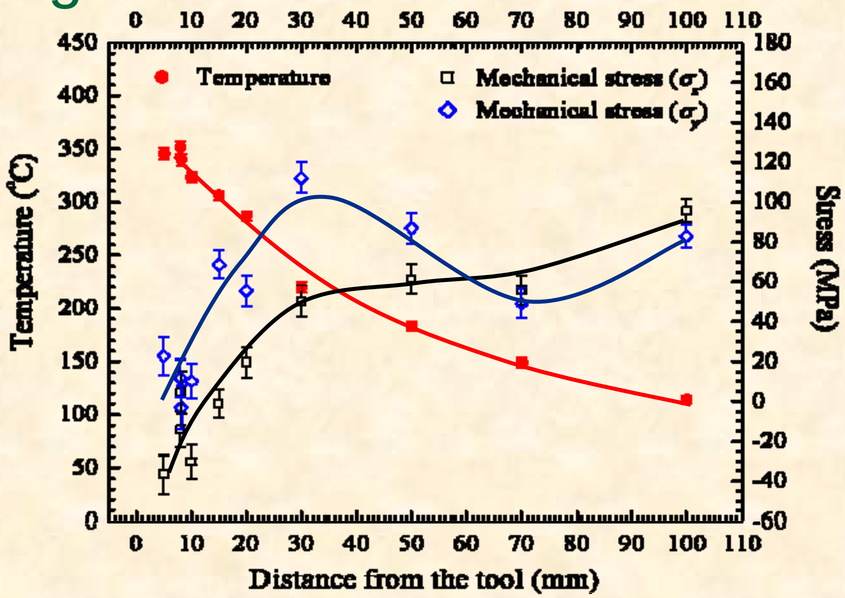

VULCAN Technical Data

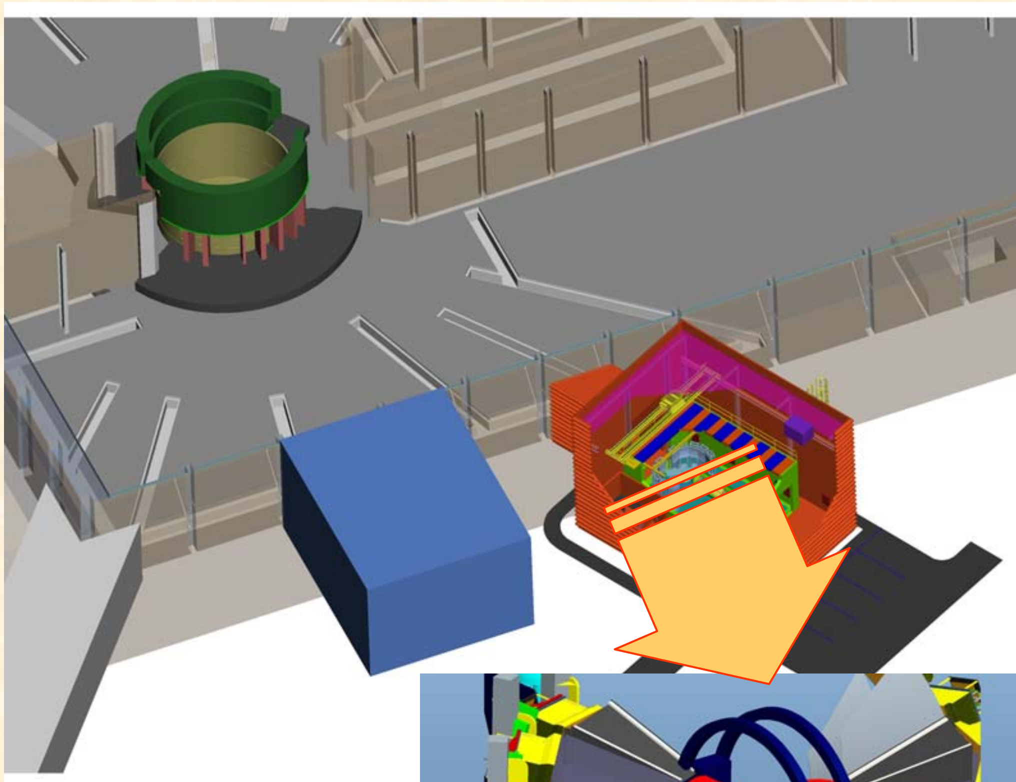

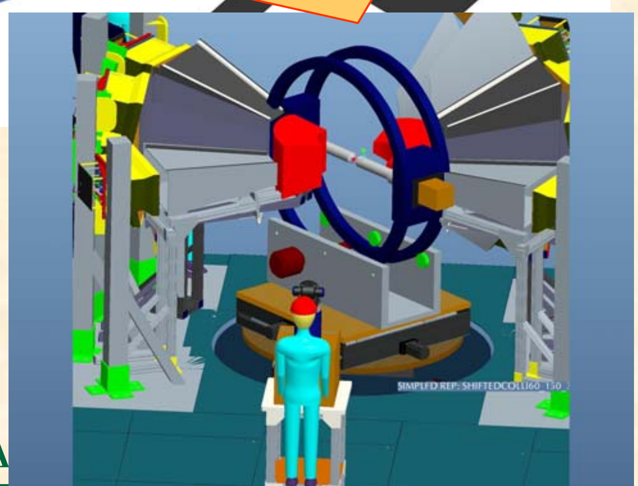

- **Flight paths**
  - **Incident ~ 43.5 m**
  - **Scatting ~ 2 m**
- **Satellite building**
- **Resolution ~ 0.2%**
- **λ ~ 0.9-3.5 Å**
- **Flux on sample (n/s/cm²/Å)**
  - **3×10^7 in high-reso. mode**
  - **1.2×10^8 in high-int. mode**
- **Wide angle detector coverage, 60-150°**
- **SANS Q-range**
  - **0.01 – 0.2 Å^{-1}**

Summary

- **Next generation neutron scattering instruments, with high flux, will lead to major breakthroughs in our understanding and, ultimately, the control of structural evolution in materials.**